

Morphometric and functional MRI changes in essential tremor with and without resting tremor

Valentina Nicoletti · Paolo Cecchi · Daniela Frosini · Ilaria Pesaresi ·
Serena Fabbri · Stefano Diciotti · Ubaldo Bonuccelli · Mirco Cosottini ·
Roberto Ceravolo

Received: 25 September 2014/Revised: 2 December 2014/Accepted: 22 December 2014/Published online: 9 January 2015
© Springer-Verlag Berlin Heidelberg 2015

Abstract The etiopathogenesis of essential tremor (ET) is still debated, since the predominant role of circuit dysfunction or brain degenerative changes has not been clearly established. The relationship with Parkinson's Disease (PD) is also controversial and resting tremor occurs in up to 20 % of ET. We investigated the morphological and functional changes associated with ET and we assessed potential differences related to the presence (ET+R) or absence (ET–R) of resting tremor. 32 ET patients (18 ET+R; 14 ET–R) and 12 healthy controls (HC) underwent 3T-MRI protocol including Spoiled Gradient T1-weighted sequence for Voxel-Based Morphometry (VBM) analysis and functional MRI during continuous writing of “8” with right dominant hand. VBM analysis revealed no gray and white matter atrophy comparing ET patients to HC and ET+R to ET–R patients. HC showed a higher BOLD

response with respect to ET patients in cerebellum and other brain areas pertaining to cerebello-thalamo-cortical circuit. Between-group activation maps showed higher activation in precentral gyrus bilaterally, right superior and inferior frontal gyri, left postcentral gyrus, superior and inferior parietal gyri, mid temporal and supramarginal gyri, cerebellum and internal globus pallidus in ET–R compared to ET+R patients. Our findings support that the dysfunction of cerebello-thalamo-cortical network is associated with ET in absence of any morphometric changes. The dysfunction of GPi in ET+R patients, consistently with data reported in PD resting tremor, might suggest a potential role of this structure in this type of tremor.

Keywords Essential tremor · Functional MRI · Voxel-based morphometry · Cerebellum

Electronic supplementary material The online version of this article (doi:10.1007/s00415-014-7626-y) contains supplementary material, which is available to authorized users.

V. Nicoletti · D. Frosini · U. Bonuccelli · R. Ceravolo (✉)
Department of Clinical and Experimental Medicine,
University of Pisa, via Roma 67, 56126 Pisa, Italy
e-mail: robertoceravolo66@gmail.com

P. Cecchi · I. Pesaresi · S. Fabbri
Neuroradiology Unit, S. Chiara Hospital, Pisa, Italy

S. Diciotti
Department of Electrical, Electronic and Information
Engineering, “Guglielmo Marconi” University of Bologna,
Cesena, Italy

M. Cosottini
Neuroradiology Unit, Department of Translational Research
and of New Surgical and Medical Technologies,
University of Pisa, Pisa, Italy

Introduction

Essential Tremor (ET) is a common neurological disorder whose etiology and pathogenesis is still debated, since the predominant role of circuit dysfunction or brain degenerative changes has not been clearly established. Several clinical [1, 2] and electrophysiological [3, 4] evidence are converging on an involvement of the cerebellum in ET, which is also suggested by several functional neuroimaging studies [5–8] revealing an increased bilateral cerebellar activity. Morphological MRI studies performed using Voxel-based morphometry (VBM) analysis provided widespread abnormalities in gray matter (GM) and white matter (WM) both in cerebellum and cerebral hemispheres, however, their results were controversial [9, 10]. From a pathological point of view, 75 % of the ET patients [11] exhibited structural changes in cerebellum although more

recently some authors raised doubts about the presence of these morphological abnormalities [12]. Further, the relationship between ET and PD is intriguing and still debated. Indeed, personal and family history of ET is commonly reported in PD patients [13], 20 % of ET patients develop resting tremor clinically similar to resting tremor in PD [14] and 25 % of ET patients might show Lewy body pathology in the locus coeruleus [11].

Hence, in this study, we investigated cerebellar function in ET patients in an exploratory design by fMRI during a specific motor task, characterized by the “8” figure writing, which strongly activates cerebellum as well as cortical motor, premotor, posterior parietal areas and thalamus [15].

We also investigated cerebellar morphometry by structural MR Imaging to assess the presence of any degenerative changes. Finally, we wished to look at the potential functional and morphological differences between ET with and without resting tremor.

Methods

Patients

Thirty-two ET patients [17 males and 15 females; 69.7 ± 9.7 years; mean values \pm Standard Deviation (SD)] were recruited at the Movement Disorders Center of Neurology Unit, University of Pisa. All patients had a diagnosis of definite or probable ET according to the Consensus Statement on tremor of Movement Disorder Society [16]. Exclusion criteria were: thyroid dysfunctions, severe vascular encephalopathy, recent brain injuries, structural lesions potentially related to tremor or history of tremorogenic drugs use. Patients were grouped into subjects with resting tremor (ET+R) and without resting tremor (ET–R) according to the score (at least 1 for ET+R and 0 for ET–R patients) in any rest tremor item for head, trunk, upper and lower extremities in the part A of Tolosa–Fahn–Marin Rating Scale (TRS) [17]. Demographic characteristics of patients are reported in Table 1. All ET+R subjects performed a ^{123}I -FP-CIT SPECT which excluded a nigrostriatal dopaminergic degeneration. Twelve healthy volunteers (4 males and 8 females; 67.4 ± 4.8 years) with no history of neurological or psychiatric diseases were recruited as controls. All patients and control subjects were right-handed according to Edinburgh Handedness Inventory [18]. Each patient was directly evaluated by a neurologist expert in movement disorder on the day of the MRI exam, before the scan. In patients taking medications for tremor, drugs were stopped 7 days before the MRI scan. Thus, all patients were clinically scored in the same condition (off medication).

Age and gender did not significantly differ between patients and controls (Mann–Whitney U test $p = 0.15$ for age; Pearson Chi-square $p = 0.24$ for sex) and between ET–R and ET+R patients ($p = 0.61$ for age; $p = 0.30$ for sex); neither disease duration differed between ET–R and ET+R (Mann–Whitney U test $p = 0.17$).

Patients and controls gave their written informed consent to all the diagnostic procedures. The protocol was approved by our Ethics Committee.

MRI

MRI data were acquired on a 3.0 T scanner (Discovery MR750 3.0 T, GE Healthcare, Milwaukee) with high-performing gradients (strength 50 mT/m, maximum slew rate 200 T/m/s) equipped with an eight channels head coil with ASSET technology. Foam cushions were used for head stabilization to reduce motion-related artifacts. All participants underwent the same MRI protocol with structural and functional acquisition in the same session for each subject.

Voxel-based morphometry

After scouts, a high-resolution fast 3D Spoiled Gradient Recalled (SPGR) sequence was acquired on axial plane (TR = 8.2 ms; TE = 3.2 ms; flip angle = 12° ; TI = 450 ms; FOV = 25.6 cm; 256×256 matrix; 160 slices; slice thickness 1.0 mm). The VBM analysis was carried out by the FSL-VBM optimized protocol [19] available in the FMRIB software library (FSL). Structural images were brain-extracted using Brain Extraction Tool (BET) [20] and manually refined. Then, these images were segmented into GM using FMRIB’s Automated Segmentation Tool (FAST) [21], aligned to the Montreal Neurological Institute (MNI) 152 standard space [22] by the affine registration tool FMRIB’s Linear Image Registration Tool (FLIRT) [23, 24] and subsequently non-linearly registered using FMRIB’s Nonlinear Image Registration Tool (FNIRT) [25]. To create a study-specific template, the registered GM images of 10 healthy subject and 10 ET patients were averaged. After that the native GM images of all subjects were non-linearly registered to the study-specific template, modulated and smoothed with an isotropic Gaussian kernel with a sigma of 3 mm. Statistical analysis was performed using a voxel-wise General Linear Model (GLM) with a permutation-based (5,000 permutations) non-parametric testing and Threshold-Free Cluster Enhancement option (TFCE) [26]. The significance level was set at $p < 0.05$ corrected for multiple comparisons via family-wise error correction across space.

To further assess possible differences in GM volume between ET–R and ET+R patients, a second study-

Table 1 Demographic and clinical data

| | Patients | | |
|--------------------------------|-------------|-------------------------------|--|
| | Total | ET–R | ET+R |
| Number # | 32 | 14 | 18 |
| Age | 69.7 ± 9.7 | 68.6 ± 8.7 | 70.5 ± 10.6 |
| Gender | 17 M/15F | 6 M/8F | 11 M/7F |
| Disease duration | 13.4 ± 12.9 | 9.9 ± 10.6 | 16.1 ± 14.2 |
| Age of onset | 56.3 ± 5.5 | 58.7 ± 9.6 | 54.4 ± 21.4 |
| Patients with family history # | 17 | 7 | 10 |
| Patients on therapy # | 13 | 6 | 7 |
| Type of therapy | | 4 Propranolol 2 Gabapentin | 5 Propranolol 1 Gabapentin 1 Zonisamide |
| TRS | 25.6 ± 9.5 | 19.4 ± 5.4* | 30.4 ± 9.8* |
| Dystonic features | – | – | – |
| Resting tremor distribution | – | – | 4 left UL 7 right UL 4 both UL 1 left UL + left LL 1 both UL + both LL 1 both UL + right LL |

Mean ± standard deviation (SD)

UL upper limb, LL lower limb

* $p < 0.001$ Mann–Whitney

U test

specific template was created with the registered GM images of 10 ET–R patients and 10 ET+R patients and then we performed the analysis as described above. Since voxel-based quantification of atrophy is influenced by aging [27], we inserted age and gender of patients and controls as covariate variables within the GLM matrix.

Functional magnetic resonance imaging

Study protocol

We used a block-design experiment with five task periods lasting 30 s each alternated to five rest periods with the same duration. Subjects were asked to perform a continuous writing of the “8” figure with their right dominant hand and to maintain self-paced frequency and amplitude as constant as possible during the experiment. Subjects were trained to the task before the exam out of the scanner and also within the magnet before fMRI acquisitions to check the capability to perform a corrected task. They also were invited to maintain the eyes closed for the whole experiment because it restricts the risk of motion artifacts and particularly because the oculomotor activity could interfere with the cerebellar activation [28]. The task execution was externally guided by the auditory inputs “go” and “stop” and monitored in real-time by a compatible device previously developed [15]. The device allowed to monitor possible errors throughout the active or passive phases of the task and to evaluate, for each subject, the

mean frequency and the mean size of the “8” figures. These parameters exert a significant effect on BOLD activation within primary sensory, motor and premotor frontal cortices (frequency) and in posterior parietal cortex (size); both frequency and size parameters modulate activation in the inferior cerebellum [15].

fMRI data acquisition

The fMRI data were obtained with a T2*-weighted gradient recalled multi-phase Eco-Planar Imaging (EPI) sequence, with the following parameters: TR 3,000 ms, TE 40 ms, flip angle 90°, FOV 26.0 cm, image matrix $\times 128 \times 128$. 28 interleaved slices (slice thickness 4 mm, spacing 1 mm) were acquired angled of 30° with respect to the anterior–posterior commissural plane (AC–PC) to minimize susceptibility-related artifacts, repeated over 104 volumes for a total scanning time of 5 min and 12 s.

fMRI data analysis

Functional data were analyzed using FEAT tool part of FSL. To avoid T1-related relaxation effects, the first four scans of each run were discarded from analysis. Pre-statistics processing consisted of motion correction using MCFLIRT [23, 24], slice-timing correction (interleaved acquisition), non-brain structures removal using BET [20], high pass temporal filtering (cut off = 100 s) and spatial

smoothing (Gaussian kernel Full Width Half Maximum = 8 mm). Subjects with absolute translational or rotational displacement higher than 3 mm or 3° were excluded from further analysis.

First-level statistical analysis was performed by GLM approach also including, in the design matrix, the head motion parameters estimated by MCFLIRT as adjunctive confound variables. BOLD activation maps were obtained comparing signal changes between active versus rest phases for each subject. Functional data were registered to brain-extracted refined 3D T1-weighted SPGR images by FLIRT [23] and subsequently both functional and structural data were aligned to the MNI 152 standard space using FNIRT [25]. The Z statistical maps resulting from the first-level analysis underwent voxel-based correction with a threshold set to $p = 0.001$.

To reveal statistically significant differences in BOLD signal between active and rest phases within the group of patients and controls, a single-tail t test was performed by a fixed-effects model [29, 30]. The Z statistical maps derived from within-group analysis underwent cluster thresholding with Z threshold = 10 and a (corrected) cluster significance threshold of $p = 0.001$.

Between-group analysis was later performed to reveal possible differences in BOLD activation pattern between patients and controls using unpaired t test and a fixed-effects model. The Z statistical maps underwent cluster thresholding with Z threshold = 5 and a (corrected) cluster p threshold = 0.001.

Finally, a further between-group analysis was performed between ET+R patients group and ET–R patients group. The Z statistical maps obtained underwent cluster thresholding with Z threshold = 5 and a (corrected) cluster p threshold = 0.001.

Age and gender of patients and controls were inserted as covariate variables in all the GLM models [27]. To remove the contribution of the variability in task performance to the cortical activation mean frequency and size of “8”, figures were included, for each subjects, in the analysis as confound variables. GM probability maps were also added to the models to include voxel-wise tissue information as nuisance variable [31]. The description of statistical maps was based on Anatomical Automated Labeling (AAL) Atlas [32].

Results

Clinical data

No significant differences were found in clinical characteristics of the two subgroups with the exception of TRS score which was, as expected, significantly higher in

ET+R patients with respect to ET–R patients. Some subjects did not drink any alcohol so we were not able to evaluate possible differences in alcohol sensitivity between groups. Similarly, some subjects did not assume any drugs for tremor, but no significant difference was found in the number of patients taking and not taking medication between ET–R and ET+R.

Behavioral data

All patients and controls correctly performed the writing of the “8” figure. ET patients performed “8” figure writing task with a mean frequency significantly different (Mann–Whitney U test $p < 0.05$) with respect to controls (0.48 vs 0.63 Hz, respectively), whereas mean area (815 vs 603 mm²) did not differ between the two groups. No significant differences were found in the task’s features by comparing ET–R and ET+R (Mann–Whitney U test; $p = 0.15$ for frequency, $p = 0.21$ for size). Plots of the frequency and the size of the “8” figures performed by healthy controls, ET patients and subgroups of ET+R and ET–R patients are available as supplemental materials (see Online Resource 1 and 2).

Voxel-based morphometry

The between-group VBM analysis revealed no significant differences in cortical GM volume both between ET patients and healthy controls and between ET–R and ET+R patients.

fMRI analysis

Within-group analysis

When comparing active and rest periods, ET patients showed significant bilateral activation in precentral gyrus, superior, middle and inferior frontal gyri, supplementary motor area (SMA), Rolandic operculum, postcentral gyrus, superior and inferior parietal gyri, supramarginal gyrus. Activation in these areas was more widespread on the left side, contralaterally to the task. A significant activation in left cinguli gyrus was also observed. ET patients presented significant bilateral activation in cerebellar hemispheres and vermis, which was more widespread on the right side, ipsilaterally to the task. The same cerebral and cerebellar areas presented significant activation in healthy controls by comparing active with rest periods. Similarly, activated clusters were more widespread on the left side in cerebral areas and on the right side in cerebellar regions. However, control subjects showed also significant left thalamus activation which was not revealed in ET patients.

Between-group analysis

Healthy subjects showed significant higher activation with respect to ET patients in precentral and postcentral gyrus bilaterally (with more extension on the left side), in left SMA, cinguli gyrus and inferior parietal gyrus. Also, left thalamus was significantly more activated in controls compared to ET patients. Further, in healthy subjects, higher activated clusters were found in cerebellum bilaterally, mainly on the right side. In a lesser extent, left superior frontal gyrus and superior parietal gyrus, right middle frontal gyrus and supramarginal gyrus, resulted more activated in controls compared to ET patients (Table 2; Fig. 1).

By comparing ET patients to healthy subjects, little clusters of significant higher activation were detected in left precentral and postcentral gyrus, precuneus and superior parietal gyrus (Table 2; Fig. 1).

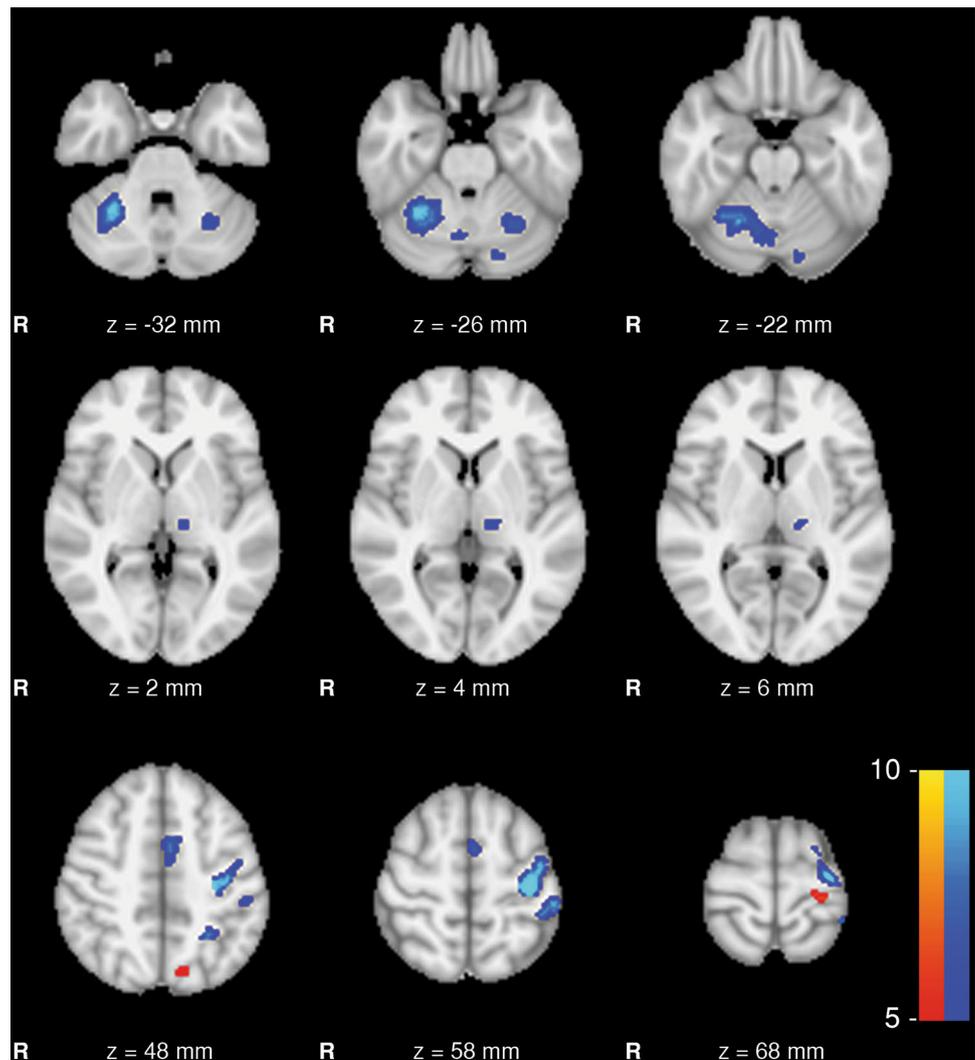
A significantly higher activation in ET–R patients with respect to ET+R patients was observed in precentral gyrus bilaterally (more widespread on the left side), in left postcentral gyrus, supramarginal gyrus, superior and inferior parietal gyri and medium temporal gyrus. In a lesser extent, right superior and inferior frontal gyri and left cerebellum resulted more activated in ET–R patients. A significant higher activation was also shown in left internal globus pallidus (GPi) (Table 3; Fig. 2).

Table 2 Results of the between-group analysis during “8” figure writing task

| AAL anatomical area | | Activated (mm ³) | Z max | MNI coordinates | | |
|--|-------------------|------------------------------|-------|-----------------|--------|--------|
| | | | | x (mm) | y (mm) | z (mm) |
| Healthy controls vs ET patients | | | | | | |
| Frontal lobes | | | | | | |
| 1 | Precentral_L | 4,856 | 12.6 | –34 | –20 | 62 |
| 2 | Precentral_R | 280 | 6.8 | 62 | 4 | 36 |
| 3 | Frontal_Sup_L | 280 | 6.3 | –28 | –10 | 68 |
| 8 | Frontal_Mid_R | 208 | 6.7 | 44 | –6 | 54 |
| 19 | Supp_Motor_Area_L | 1,384 | 7.6 | –4 | 2 | 50 |
| 33 | Cingulum_Mid_L | 264 | 6.5 | –4 | –2 | 48 |
| Parietal lobes | | | | | | |
| 57 | Postcentral_L | 2,984 | 11.1 | –36 | –22 | 54 |
| 58 | Postcentral_R | 632 | 6.9 | 44 | –28 | 36 |
| 59 | Parietal_Sup_L | 152 | 7.1 | –24 | –50 | 46 |
| 61 | Parietal_Inf_L | 1,312 | 9.1 | –42 | –26 | 38 |
| 64 | SupraMarginal_R | 240 | 6.9 | 46 | –28 | 36 |
| Thalamus | | | | | | |
| 77 | Thalamus_L | 264 | 5.7 | –12 | –22 | 4 |
| Cerebellum | | | | | | |
| 91 | Cerebelum_Crus1_L | 368 | 6.1 | –16 | –78 | –26 |
| 92 | Cerebelum_Crus1_R | 440 | 6.9 | 34 | –54 | –34 |
| 98 | Cerebelum_4_5_R | 896 | 7.5 | 16 | –56 | –18 |
| 99 | Cerebelum_6_L | 1,208 | 7.0 | –28 | –60 | –26 |
| 100 | Cerebelum_6_R | 5,536 | 10.9 | 30 | –52 | –30 |
| 104 | Cerebelum_8_R | 1,792 | 7.4 | 30 | –62 | –54 |
| 112 | Vermis_6 | 832 | 7.1 | 2 | –70 | –16 |
| 113 | Vermis_7 | 56 | 5.5 | 6 | –66 | –26 |
| ET patients vs healthy controls | | | | | | |
| Frontal lobes | | | | | | |
| 1 | Precentral_L | 128 | 6.5 | –24 | –26 | 68 |
| Parietal lobes | | | | | | |
| 57 | Postcentral_L | 184 | 6.6 | –28 | –28 | 68 |
| 59 | Parietal_Sup_L | 104 | 5.7 | –14 | –72 | 50 |
| 67 | Precuneus_L | 128 | 5.8 | –12 | –72 | 48 |

AAL Anatomical Automated Labeling Atlas, MNI Montreal Neurological Institute

Fig. 1 Results of the between-group (healthy controls and ET patients) comparison activation map. Maps of higher activated clusters in healthy controls compared to ET patients (*blue*) and in ET patients compared to healthy controls (*red*) superimposed on standard MNI template (Z threshold >5 ; cluster p threshold <0.001)



ET+R patients did not show any significant more activated clusters with respect to ET–R patients.

Discussion

Our study did not show any significant GM loss either in cerebellum or in other cerebral areas. This finding is consistent with some previous VBM studies performed in ET patients both with 1.5T [33] and 3T magnets [34, 35]. Nevertheless, it is conflicting with other studies which revealed widespread neocortical areas of atrophy [9, 10]. Some authors found GM loss in cerebellar vermis only in the ET patients' subgroup with head tremor but not in the whole cohort of ET patients [36, 37].

As expected, the “8” figure writing evoked activation, in both patients and controls, in cerebellum and primary sensorimotor cortex as other simple motor tasks. Premotor cortex, SMA, cinguli gyrus and posterior parietal areas

were also activated in relation to the increased complexity of the task. In controls but not in ET patients, the task evoked activation also in left thalamus.

The between-group analysis revealed clusters of higher activation in controls with respect to ET patients in cerebellar hemispheres, particularly on the right side. The lobules VI and VIII, which are related to motor and somatosensory functions of cerebellum, were the widest activated areas. Thus, ET patients showed a dysfunction of cerebellum which is not explained by atrophy as confirmed by VBM analysis. However, ET patients showed less activation compared to controls also in left primary sensorimotor area, frontal superior gyrus, SMA, parietal inferior gyrus and left thalamus (posterior ventral lateral region). The reduced recruitment of all these areas in ET with respect to controls is unrelated to atrophy but it might be due to a dysfunction along the cerebello-thalamo-cortical network (Fig. 3). Actually the brain areas whose activation was higher in controls than in ET patients,

Table 3 Results of the between-group analysis in ET–R compared to ET+R patients

| AAL anatomical area | | Activated (mm ³) | Z max | MNI coordinates | | |
|---------------------|--------------------|------------------------------|-------|-----------------|--------|--------|
| | | | | x (mm) | y (mm) | z (mm) |
| Frontal lobes | | | | | | |
| 1 | Precentral_L | 744 | 7.5 | –28 | –28 | 66 |
| 2 | Precentral_R | 464 | 7.1 | 64 | 10 | 24 |
| 6 | Frontal_Sup_Orb_R | 392 | 6.4 | 18 | 24 | –16 |
| 12 | Frontal_Inf_Oper_R | 120 | 6.1 | 62 | 12 | 28 |
| 16 | Frontal_Inf_Orb_R | 184 | 6.3 | 18 | 20 | –18 |
| Parietal lobes | | | | | | |
| 57 | Postcentral_L | 1,640 | 8.2 | –28 | –30 | 64 |
| 59 | Parietal_Sup_L | 480 | 7.2 | –26 | –54 | 66 |
| 61 | Parietal_Inf_L | 168 | 6.9 | –60 | –24 | 46 |
| 63 | SupraMarginal_L | 832 | 7.2 | –64 | –22 | 38 |
| Pallidum | | | | | | |
| 75 | Pallidum_L | 80 | 5.8 | –12 | 0 | –6 |
| Temporal lobes | | | | | | |
| 85 | Temporal_Mid_L | 480 | 6.3 | –50 | –48 | –4 |
| Cerebellum | | | | | | |
| 91 | Cerebellum_Crus1_L | 56 | 5.5 | –30 | –78 | –20 |
| 99 | Cerebellum_6_L | 240 | 6.0 | –28 | –76 | –20 |

AAL Anatomical Automated Labeling Atlas, MNI Montreal Neurological Institute

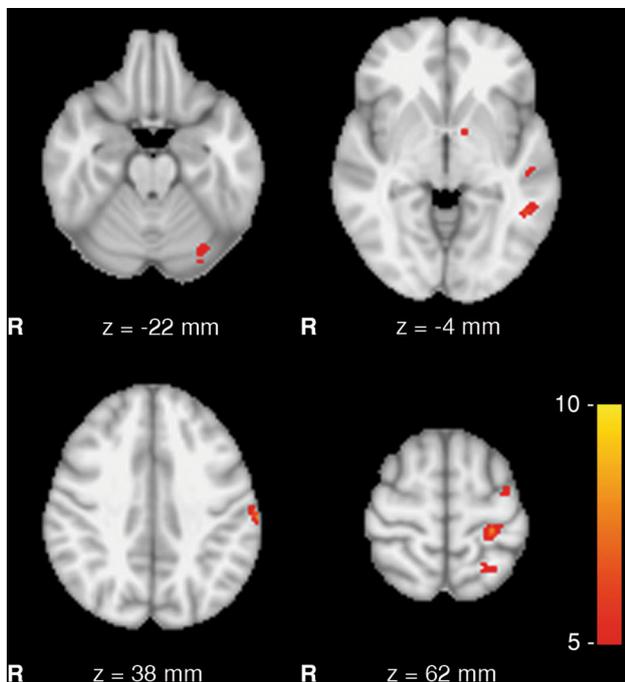


Fig. 2 Results of the between group (ET–R and ET+R patients) comparison activation map. Map of higher activated clusters in ET–R compared to ET+R patients (red) superimposed on standard MNI template (Z threshold >5; cluster *p* threshold <0.001)

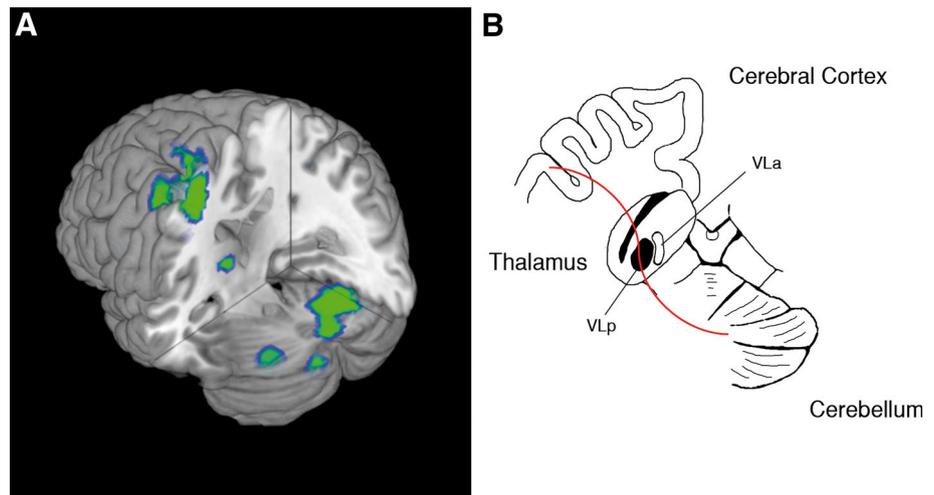
belong to this circuit according to the evidence from previous electrophysiological studies. To account for variability in task performance, we inserted mean value of

frequency and size of “8” figures performed by each subject as adjunctive explanatory variable in the statistical model. In this way, BOLD signal difference between controls and patients was independent of the differences in task performance by the two groups.

High-resolution magnetoencephalography (MEG)-electromyography (EMG) coherence studies recently confirmed the role of cerebello-thalamo-cortical network in ET and in other movement disorders characterized by tremor. In ET patients, a coherent activity at tremor frequency between EMG signal and MEG recorded by primary motor cortex has been reported and interestingly a cortico-cortical coherence activity between M1 and ipsilateral premotor area, thalamus and contralateral cerebellum and brainstem was detected [38]. Similar results were found in patients affected from Wilson’s Disease with postural/intentional tremor [39], in resting tremor in PD [40] as well as in physiologic tremor [41] and “voluntary” tremor [42]. Hence, the dysfunction of this network, physiologically active in healthy subjects during the execution of rhythmic and repetitive voluntary precision movements [43], could presumably generate tremor. Recently, two resting-state fMRI (RS-fMRI) studies have shown impaired functional connectivity within the cerebello-thalamo-cortical network in ET patients with respect to healthy controls using both independent component analysis [44] and regional homogeneity measurement [35].

Several evidence, although not univocally [45], reported the crucial role of thalamus as drive of this network. In

Fig. 3 Cerebello-thalamo-cortical network. 3D image of the network found in our fMRI study by comparing healthy subjects with ET patients (a) and its schematic representation (b). In b, *VLP* ventrolateral posterior thalamic nucleus; *VLa* ventrolateral anterior thalamic nucleus



drug-resistant ET, neurons of VIM, which receives the main cerebellar projections, presented a frequency discharge proportional to EMG signal recorded from contralateral forearm maintained in antigravitary position [46, 47]. Our finding that in ET patients the motor task, differently from controls, was not able to evoke activation in left thalamus, could support the role of thalamic dysfunction in the generation of tremor in ET. However, our study could not allow us to establish if thalamus is the primary drive of this circuit. Its importance has been suggested by a recent electrophysiological study which analyzed the interaction between thalamus and motor cortex within the cerebello-thalamo-cortical network in patients with voluntary tremor compared to those with involuntary tremor. In the former thalamus mainly relayed motor-related information to cortex, whereas in the latter a bidirectional mode of interaction was detected [42]. On the other hand, also cerebellum seems to play an important role [3, 5–8] and electrophysiological studies have also shown the involvement of motor cortex, although intermittent [48, 49]. Further, a simultaneous activation of all the network components in ET has been previously reported [38] and an ischemic lesion in any component of the circuit could reduce ET in single patients [50]. All these data have led to the hypothesis of a dynamic entrainment between the network structures which may all act as oscillator [51], in absence of a unique primary drive.

Nevertheless, the dysfunction of cerebello-thalamo-cortical circuit reported in ET patients during the execution of a motor task in our study suggests that there is an impairment in the individual components of this network. Previous PET studies have shown the crucial role of GABAergic modulation in key structures of this circuit [52, 53]. In ET, a reduction in the GABAergic output of cerebellar Purkinje cells could reduce the inhibitory activity on

the deep cerebellar nuclei neurons with an increased cerebellar output towards the thalamic and cortical stations of the network, supporting the use of GABAergic drugs for ET. Further information could be provided by functional studies exploring GABAergic drugs' effects on this circuit.

The comparison between ET patients and controls showed, in the former, some higher activated areas in precentral and postcentral gyri and, above all, in precuneus and superior parietal gyrus. This finding could be related to an augmented integration of sensorial inputs in patients during the writing task. However, precuneus, which shows connections with inferior parietal gyrus, could not exclusively carry out spatial functions but it could be implicated in sustained attention and identification of significant events and so probably is more activated in ET patients since for the complexity of the task they could require additional effort with respect to controls.

The comparison between ET+R patients and ET–R patients showed, in the latter, a major activation especially in contralateral sensorimotor cortex, superior parietal gyrus and supramarginal gyrus. It could be related to the fact that the presence of resting tremor in ET+R patients could produce an increased BOLD effect during the rest phase of the task with respect to ET–R patients, who did not have any tremor in rest phase. So when BOLD effect of the rest phase was deducted from BOLD effect of the active phase of the task, signal change was lower in ET+R group compared to ET–R group. Interestingly, ET–R patients presented an increased GPi activation in comparison to ET+R patients suggesting a GPi dysfunction in ET+R patients. GPi has just been retained implicated in resting tremor generation in Parkinson's Disease (PD). Actually in an EMG-fMRI study [54], a correlation between activity in the cerebello-thalamo-cortical network and the amplitude of resting tremor was reported, while GPi has been

proposed as a trigger in the generation of a pathological oscillatory activity within the cerebello-thalamo-cortical network. The authors found also a positive correlation between clinical severity of tremor and dopamine depletion of GPi measured by [I-123]FP-CITSPECT. The role of GPi in PD tremor has been suggested by several imaging [55], electrophysiological [56], and pathological studies in humans [57] and primates [58, 59]. On the other hand, a recent postmortem study reported near-normal dopamine levels in ventral GPi of PD patients with prominent tremor [60]. No evidence so far on GPi in ET is available. Unfortunately, in our study, we cannot definitely establish a causal relationship between GPi dysfunction and resting tremor in part also because of the lack of a tremor quantitative analysis during the fMRI study. Thus, we could not correlate GPi activation with resting tremor severity. The evidence from our experience can only suggest a potential role of GPi in the resting component of ET, similar to resting tremor in PD.

Finally, another limitation of our study is related to the use of fixed-effects modeling in the higher level statistical analysis that could limit the generalization of our results to the entire population of ET patients.

Conclusions

Our task-related fMRI study confirmed that the dysfunction of the cerebello-thalamo-cortical network is associated with ET supporting the strong evidence from electrophysiological studies regarding the pathogenetic role of this circuit in the generation of ET. We also detected the dysfunction of GPi in ET patients with resting tremor consistently with the data reported in PD resting tremor and suggesting a potential key role of GPi in the generation of this type of tremor.

Conflicts of interest On behalf of all authors, the corresponding author states that there is no conflict of interest.

References

- Louis ED, Frucht SJ, Rios E (2009) Intention tremor in essential tremor: prevalence and association with disease duration. *Mov Disord* 24:626–627
- Singer C, Sanchez-Ramos J, Weiner WJ (1994) Gait abnormality in essential tremor. *Mov Disord* 9:193–196
- Helmchen C, Hagenow A, Miesner J et al (2003) Eye movement abnormalities in essential tremor may indicate cerebellar dysfunction. *Brain* 126(pt 6):1319–1332
- Gitchel GT, Wetzel PA, Baron MS (2013) Slowed saccades and increased square wave jerks in essential tremor. *Tremor Other Hyperkinet Mov (NY)* 3. [pii]: tre-03-178-4116-2 (eCollection 2013)
- Colebatch JC, Findley LJ, Frackowiak RS, Marsden CD, Brooks DJ (1990) Preliminary report: activation of the cerebellum in essential tremor. *Lancet* 336:1028–1030
- Jenkins IH, Bain PG, Colebatch JG et al (1993) A positron emission tomography study of essential tremor: evidence for overactivity for cerebellar connections. *Ann Neurol* 34(1): 82–90
- Boecker H, Wills AJ, Ceballos-Baumann A et al (1996) The effect of ethanol alcohol responsive essential tremor: a positron emission tomography. *Ann Neurol* 39(5):650–658
- Bucher SF, Seelos KC, Dodel RC, Reiser M, Oertel WH (1997) Activation mapping in essential tremor with functional magnetic resonance imaging. *Ann Neurol* 41(1):32–40
- Benito-Leon J, Alvarez-Linera J, Hernandez-Tamames JA, Alonso-Navarro H, Jimenez-Jimenez FJ, Louis ED (2009) Brain structural changes in essential tremor: voxel-based morphometry at 3-Tesla. *J Neurol Sci* 287:138–142
- Bagepally BS, Bhatt MD, Chandran V et al (2010) Decrease in cerebral and cerebellar gray matter in essential tremor: a voxel-based morphometric analysis under 3T MRI. *J Neuroimaging* 20:1–4
- Louis ED, Faust PL, Vonsattel JP et al (2007) Neuropathological changes in essential tremor: 33 cases compared with 21 controls. *Brain* 130:3297–3307
- Rajput AH, Robinson CA, Rajput ML, Robinson SL, Rajput A (2012) Essential tremor is not dependent upon cerebellar Purkinje cell loss. *Parkinsonism Relat Disord* 18(5):626–628
- Fekete R, Jankovic J (2011) Revisiting the relationship between essential tremor and Parkinson's disease. *Mov Disord* 26:391–398
- Cohen O, Pullman S, Jurewicz E, Watner D, Louis ED (2003) Rest tremor in patients with essential tremor: prevalence, clinical correlates, and electrophysiologic characteristics. *Arch Neurol* 60:405–410
- Diciotti S, Cecchi P, Ginestroni A et al. (2010) MR-compatible device for monitoring hand tracing and writing tasks in fMRI with an application to healthy subjects. *Conc Magn Reson Imaging Part A* 36A:139–152
- Deuschl G, Bain P, Brin M (1998) Consensus statement of the Movement Disorder Society on Tremor. *Ad Hoc Sci Comm Mov Disord* 13(suppl 3):2–23
- Fahn S, Tolosa E, Conception M (1993) Clinical rating scale for tremor. In: Jankovic J, Tolosa E (eds) *Parkinson's disease and movement disorders*, 2nd edn. Williams and Wilkins, Baltimore, pp 271–280
- Oldfield RC (1971) The assessment and analysis of handedness: the Edinburgh inventory. *Neuropsychologia* 9(1):97–113
- Ashburner J, Friston K (2000) Voxel-based morphometry—the methods. *Neuroimage* 11:805–821
- Smith SM, Zhang Y, Jenkinson M et al (2002) Accurate, robust and automated longitudinal and cross-sectional brain change analysis. *Neuroimage* 17:479–489
- Zhang Y, Brady M, Smith S (2001) Segmentation of brain MR images through a hidden Markov random field model and the expectation maximization algorithm. *IEEE Trans Med Imaging* 20:45–57
- Mazziotta JC, Toga AW, Evans A, Fox P, Lancaster J (1995) A probabilistic atlas of the human brain: theory and rationale for its development. *Neuroimage* 2:89–101
- Jenkinson M, Smith SM (2001) A global optimisation method for robust affine registration of brain images. *Med Image Anal* 5:143–156
- Jenkinson M, Bannister PR, Brady JM, Smith SM (2002) Improved optimisation for the robust and accurate linear registration and motion correction of brain images. *Neuroimage* 17:825–841

25. Andersson JLR, Jenkinson M, Smith S (2007) Non-linear registration, aka Spatial normalisation. FMRIB Technical Report TR07JA2 2007 from www.fmrib.ox.ac.uk/analysis/techrep
26. Smith SM, Nichols TE (2009) Threshold-free cluster enhancement: addressing problems of smoothing, threshold dependence and localisation in cluster inference. *Neuroimage* 44:83–98
27. Draganski B, Ashburner J, Hutton C et al (2011) Regional specificity of MRI contrast parameter changes in normal ageing revealed by voxel-based quantification (VBQ). *Neuroimage* 55:1423–1434
28. Glickstein M, Sultan F, Voogd J (2011) Functional localization in the cerebellum. *Cortex* 47:59–80
29. Beckmann CF, Smith S, Jenkinson M (2003) General multi-level linear modelling for group analysis in FMRI. *Neuroimage* 20:1052–1063
30. Woolrich MW, Behrens TE, Beckmann CF, Jenkinson M, Smith SM (2004) Multilevel linear modelling for FMRI group analysis using Bayesian inference. *Neuroimage* 21:1732–1747
31. Oakes TR, Fox AS, Johnstone T, Chung MK, Kalin N, Davidson RJ (2007) Integrating VBM into the general linear model with voxelwise anatomical covariates. *Neuroimage* 34:500–508
32. Tzourio-Mazoyer N, Landeau B, Papathanassiou D et al (2002) Automated anatomical labeling of activations in SPM using a macroscopic anatomical parcellation of the MNI MRI single-subject brain. *Neuroimage* 15:273–289
33. Daniels C, Peller M, Wolff S et al (2006) Voxel-based morphometry shows no decreases in cerebellar grey matter volume in essential tremor. *Neurology* 67:1452–1456
34. Klein JC, Lorenz B, Kang JS et al (2011) Diffusion tensor imaging of white matter involvement in essential tremor. *Hum Brain Mapp* 32:896–904
35. Fang W, Lv F, Luo T et al. (2013) Abnormal regional homogeneity in patients with essential tremor revealed by resting-state functional MRI. 8(7):e69199. doi:10.1371/journal.pone.0069199 (print 2013)
36. Quattrone A, Cerasa A, Messina D et al (2008) Essential head tremor is associated with cerebellar atrophy: a volumetric and voxel-based morphometry MR imaging study. *Am J Neuroradiol* 29:1692–1697
37. Cerasa A, Messina D, Nicoletti G et al (2009) Cerebellar atrophy in essential tremor using an automated segmentation method. *Am J Neuroradiol* 30(6):1240–1243
38. Schnitzler A, Munks C, Butz M, Timmermann L, Gross J (2009) Synchronized brain network associated with essential tremor as revealed by magnetoencephalography. *Mov Disord* 24(11):1629–1635
39. Sudmeyer M, Pollok B, Hefter H et al (2006) Synchronized brain network underlying postural tremor in Wilson's disease. *Mov Disord* 21(11):1935–1940
40. Timmermann L, Gross J, Dirks M, Volkmann J, Freund HJ, Schnitzler A (2003) The cerebral oscillatory network of parkinsonian resting tremor. *Brain* 126:199–212
41. Schnitzler A, Timmermann L, Gross J (2006) Physiological and pathological oscillatory networks in the human motor system. *J Physiol Paris* 99:3–7
42. Pollok B, Gross J, Dirks M, Timmermann L, Schnitzler A (2004) The cerebral oscillatory network of voluntary tremor. *J Physiol* 554:871–878
43. Gross J, Timmermann J, Kujala M et al (2002) The neural basis of the intermittent motor control in humans. *Proc Natl Acad Sci USA* 99:2299–2302
44. Popa T, Russo M, Vidailhet M et al (2013) Cerebellar rTMS stimulation may induce prolonged clinical benefits in essential tremor and subjacent changes in functional connectivity: an open label trial. *Brain stim* 6(2):175–179. doi:10.1016/j.brs.2012.04.009 Epub 2012 May 12
45. Contarino MF, Groot PF, van der Meer JN et al (2012) Is there a role for combined EMG-fMRI in exploring the pathophysiology of essential tremor and improving functional neurosurgery? *PLoS One* 7(10):e46234. doi:10.1371/journal.pone.0046234 (epub 2012 Oct 1)
46. Hua SE, Lenz FA, Zirh TA, Reich SG, Dougherty PM (1998) Thalamic neuronal activity correlated with essential tremor. *J Neurol Neurosurg Psychiatry* 64(2):273–276
47. Hua SE, Lenz FA (2005) Posture-related oscillations in human cerebellar thalamus in essential tremor are enabled by voluntary motor circuits. *J Neurophysiol* 93(1):117–127
48. Hellwig B, Haussler S, Schelter B et al (2001) Tremor-correlated cortical activity in essential tremor. *Lancet* 357:519–523
49. Raethjen J, Govindan RB, Kopper F et al (2007) Cortical involvement in the generation of essential tremor. *J Neurophysiol* 97:3219–3228
50. Dupuis MJ, Evrard FL, Jacquerye PG, Picard GR, Lermen OG (2010) Disappearance of essential tremor after stroke. *Mov Disord* 25(16):2884–2887
51. Raethjen J, Deuschl G (2012) The oscillating central network of Essential tremor. *Clin Neurophysiol* 123:61–64
52. Boecker H, Weindl A, Brooks DJ et al (2010) GABAergic dysfunction in essential tremor: an ¹¹C-Flumazenil PET study. *J Nucl Med* 51:1030–1035
53. Gironell A, Figueiras FP, Pagonabarraga J et al (2012) Gaba and serotonin molecular neuroimaging in essential tremor: a clinical correlation study. *Parkinsonism Relat Disord* 18:876–880
54. Helmich RC, Janssen MJ, Oyen WJ, Bloem BR, Toni I (2011) Pallidal dysfunction drives a cerebellothalamic circuit into Parkinson tremor. *Ann Neurol* 69(2):269–281
55. Prodoehl J, Spraker M, Corcos D, Comella C, Vaillancourt D (2010) Blood oxygenation level-dependent activation in basal ganglia nuclei relates to specific symptoms in de novo Parkinson's disease. *Mov Disord* 25(13):2035–2043
56. Hutchinson WD, Lozano AM, Tasker RR, Lang AE, Dostrovsky JO (1997) Identification and characterization of neurons with tremor-frequency activity in human globus pallidus. *Exp Brain Res* 113:557–563
57. Hirsch EC, Mouatt A, Faucheux B et al (1992) Dopamine, tremor, and Parkinson's disease. *Lancet* 340:125–126
58. Deutch AY, Elsworth JD, Goldstein M et al (1986) Preferential vulnerability of A8 dopamine neurons in the primate to the neurotoxin 1-methyl-4-phenyl-1,2,3,6-tetrahydropyridine. *Neurosci Lett* 68:51–56
59. Jan C, Francois C, Tande D et al (2000) Dopaminergic innervation of the pallidum in the normal state, in MPTP-treated monkeys and in parkinsonian patients. *Eur J Neurosci* 12:4525–4535
60. Rajput AH, Sitte HH, Rajput A (2008) Globus pallidus dopamine and Parkinson motor subtypes: clinical and brain biochemical correlation. *Neurology* 70(16 Pt 2):1403–1410